Optimizing the Preparation Conditions of Silica Supported Fe-Co-Ce Ternary Catalyst for the Fixed-bed Fischer-Tropsch Synthesis: Taguchi Experimental Design Approach

M. Mohammad Rezapour[a], A.A. Mirzaei[a,*] and H. Zohdi-Fasaei[b,*]

[a]*Department of Chemistry, Faculty of Sciences, University of Sistan and Baluchestan, P. O. Box: 98135-674, Zahedan, Iran*
[b]*Department of Chemical Engineering, Faculty of Engineering, University of Sistan and Baluchestan, P. O. Box: 98164-161, Zahedan,*
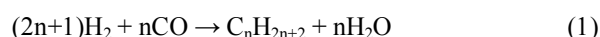
Iran

Using wet impregnation method, a novel ternary system of silica supported Fe-Co-Ce catalyst was prepared. Preparation conditions such as impregnation time and temperature, drying time and temperature were optimized by the L_9 Taguchi experimental design to achieve a light olefin selective catalyst with maximum CO conversion in a fixed bed micro-reactor. It was found that the best conditions to maximize the responses were obtained at 4 h impregnation time, 60 °C impregnation temperature, 6 h drying time, 90 °C drying temperature and 350 °C of reaction's temperature. Characterization of the optimal catalyst precursors and calcined samples before and after the Fischer-Tropsch reaction was carried out using various techniques.

INTRODUCTION

Heterogeneous catalysts are widely used in many important and industrially relevant reactions such as hydrogenation, dehydrogenation, isomerization, catalytic cracking, reforming and Fischer-Tropsch synthesis (FTS) [1-3]. FTS has attracted a great attention as a process for the production of valuable chemicals, light olefins and environment-friendly liquid fuels [4,5]. It directly converts synthesis gas (mixture of hydrogen and carbon monoxide) into hydrocarbons and clean fuels free from Sulfur and Nitrogen. The main reactions in the FTS can be expressed by Eqs. (1) and (2):

$$(2n+1)H_2 + nCO \rightarrow C_nH_{2n+2} + nH_2O \qquad (1)$$

$$2nH_2 + nCO \rightarrow C_nH_{2n} + nH_2O \qquad (2)$$

Iron and cobalt are mainly used as the active transient metals in the FTS catalysts [6], because the cost, activity and selectivity have been developed for industrial applications. Other usual metals in the FTS are Nickel, Ruthenium and Cerium [7-9]. In an iron-based FTS, light olefin selectivity usually increases at high temperatures. On the other hand, most of the products in the Cobalt-based FTS are linear and high molecular weight alkanes [10-14]. Studies on iron catalysts have shown that adding a small amount of cobalt to iron significantly increases the activity of catalysts. The mixed oxides of the two metals are more active than each metal alone [15]. The effect of using cerium as a promoter in the Fischer-Tropsch (FT) catalysts is to produce heavy hydrocarbon molecules and liquid fuels. Particularly, the resulted fuel from cerium catalyst can decrease contamination through reduction in output nitrogen impurities. It has been reported that a mixture of the Fe and Co catalysts (Fe-Co bimetallic catalysts) can significantly increase catalyst activity [10-14]. Olefin and paraffin

---

*Corresponding author. E-mail: mirzaei@hamoon.usb.ac.ir

production are the main reactions in the FTS [8]. These reactions commercially take place at the two usual modes. The first one is the low-temperature Fischer-Tropsch (180-250 ℃) over iron or cobalt catalysts, producing high molecular mass linear paraffin; indeed its water-gas shift (WGS) activity is low. The second one is the high-temperature Fischer-Tropsch (300-350 ℃), used for the production of gasoline and linear low molecular mass olefins [16,17]. The FTS is an exothermic reaction so that heat released during the reaction may cause activity and selectivity reduction due to catalyst sintering, fouling and carbon deposition. Support dissipates liberated heat from FTS, reduces the temperature gradient in the FT reactors, particularly, fixed-bed reactor. Choosing supports for Fischer-Tropsch catalysts depends on several criteria, including basicity, dispersion and metal-support interaction. Silica support improves CO conversion as well as the selectivity of ethylene to how to substantially increase product [15]. The silica powders exhibit a higher resistance, high surface area; high thermal shock resistance than Al_2O_3, TiO_2 and ZrO_2 supports [8,18]. Adesina reported that SiO_2 was the optimal support for Fe-based catalysts for FTS in terms of activity and chain growth probability [19]. Design of experiment (DOE) is a powerful mathematical technique for determining the optimum conditions [20]. Through using orthogonal arrays and statistical analysis in least time and cost, Taguchi method is a promising approach to study the influence of factors in a minimum number of experiments. On the other hand, the key factor of Taguchi is "reducing variability" [21-25].

In this study, a novel Fischer-Tropsch ternary catalyst system (silica supported Fe-Co-Ce catalyst) was prepared by the wet impregnation method, and the important synthesis parameters were optimized using Taguchi design of experiment. However, this approach is frequently applied in the fields of science and industry, the number of reported works using this method is not much in the Fischer-Tropsch synthesis. The catalyst characterization was carried out using different methods, including X-ray diffraction (XRD), Brunaur-Emmett-teller (BET) surface area, and Scanning Electron Microscopy (SEM).

MATERIALS AND METHOD

Preparation Procedure

Support synthesis. The steps of Sol-gel method for the synthesis of high specific surface area silica powders are shown in Fig. 1. Sodium silicate solution (Na_2SiO_3) (10%) was prepared, and the 1 M hydrochloric acid (HCl, Merck) solution was added drop wise into the water glass solution for 30 min (50 ml). During the neutralization of a sodium silicate solution, gelation happens typically rather quickly. Then, the mixture was stirred for eight hours with a magnetic bar at 250 rpm using a churner. Gels were washed with deionized water during two days for eight times to remove Na^+ ions from the system, resulting in the formation of silicic acid and a high-purity silica powders. After the washing treatment, gel was dried at 80 ℃ for 45 hours in hot air and calcined at 500 ℃ for 6 hours [26]. Figure 1 illustrates the diagram of the procedure for the silica support synthesis.

Catalyst synthesis. Catalysts were synthesized by the wet impregnation method. Aqueous solutions of $Co(NO_3)_2.6H_2O$ (0.5 M) (99% Merck), $Fe(NO_3)_3.9H_2O$ (0.5 M) (99% Merck) and $Ce(NO_3)_3.6H_2O$ (0.5 M) (99% Merck) containing 33.33% Co -33.33% Fe -33.33% Ce were prepared and 70 wt% of SiO_2 (based on the total catalyst weight) was added into the mixed solution of cobalt, iron and cerium nitrate. Then, according to L_9 Taguchi design of experiment (Table 1), the catalysts were impregnated and dried at different times and temperatures. Finally, all the catalysts were calcined at the same conditions (600 ℃ for 6 h). Table 2 shows the structure of Taguchi's orthogonal array for experiments.

Catalyst Testing

Catalysts were tested in a fixed bed tubular stainless steel micro reactor (Fig. 2). The catalyst loading and the catalyst implementation route are strongly linked with the heat of reaction, heat transfer and mass transfer. The micro reactor is suitable for controlling temperature in the Fischer-
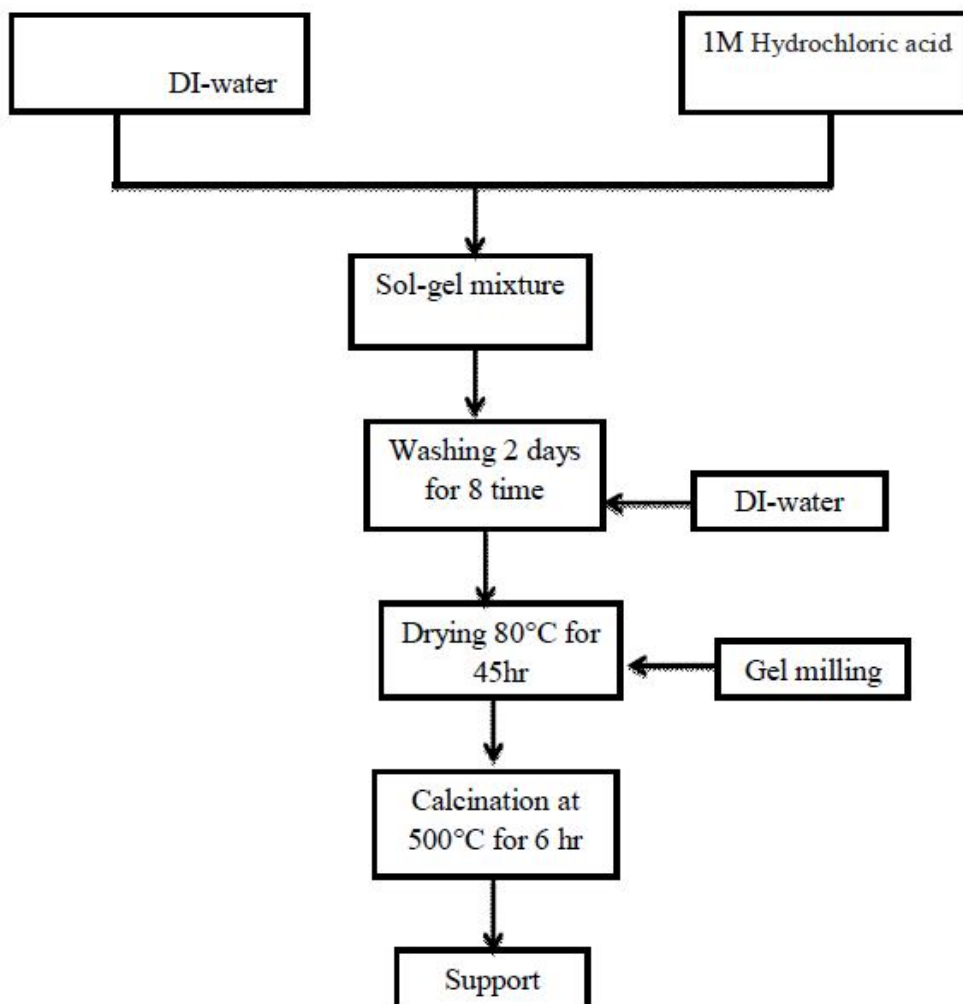
Fig. 1. The procedure for producing high specific surface area of silica powders by Sol-gel method.

Table 1. Levels of Parameters for the Catalyst Synthesis

Parameters	Level 1	Level 2	Level 3
Impregnation temperature (°C)	60	30	90
Impregnation time (h)	4	6	8
Drying temperature (°C)	90	120	150
Drying time (h)	6	15	24

Table 2. Design of Experiment According to the L_9 Orthogonal Array

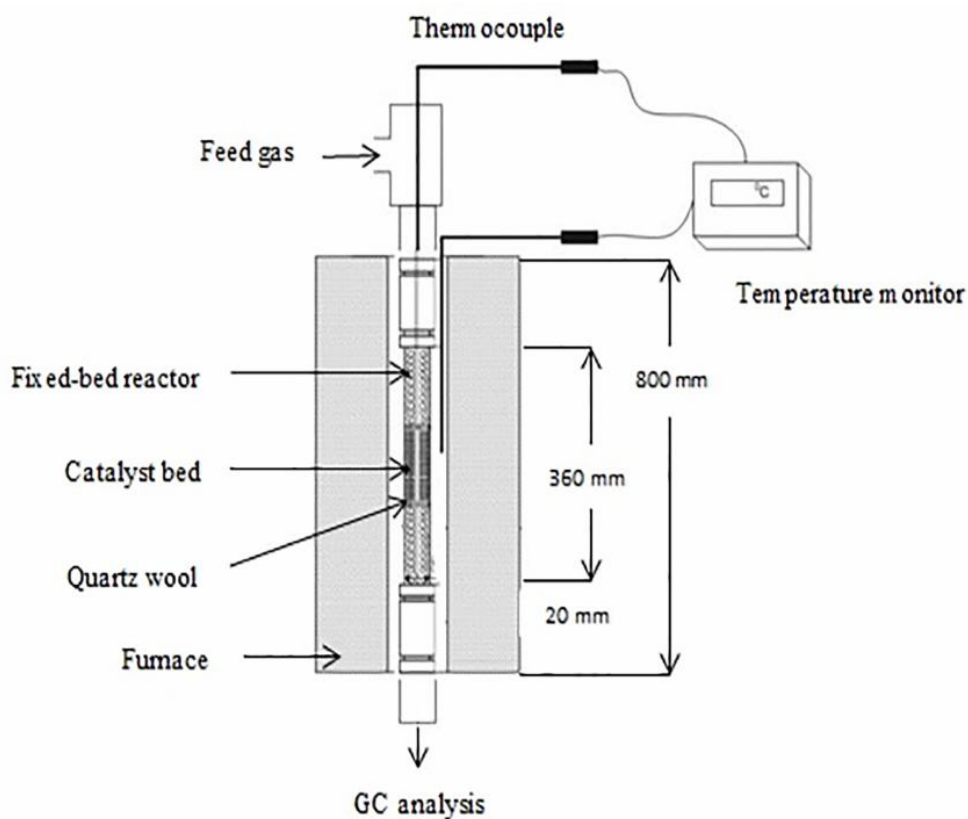| Experiment	Impregnation temperature (°C)	Impregnation time (h)	Drying temperature (°C)	Drying time (h)
1	1	1	1	1
2	1	2	2	2
3	1	3	3	3
4	2	1	2	3
5	2	2	3	1
6	2	3	1	2
7	3	1	3	2
8	3	2	1	3
9	3	3	2	1

Fig. 2. Sketch portrait of micro-fixed-bed reactor.

Tropsch reactions. The reactor was an 80 cm long stainless steel tube (diameter = 20 mm) placed in a temperature-controlled furnace and surrounded by a fiberglass to minimize heat loss. Before the catalytic tests, 1 g of powdered catalyst (dp < 250 mm) was held in the middle of the fixed bed micro reactor using quartz wool and reduced under a flow of hydrogen (H_2 = 30 ml/min) at 400 °C for 2 h. All gas lines passing through the reactor bed were made of a 1/4″ stainless steel tub. Three mass flow controllers (Brooks, Model 5850E) equipped with a four-channel read out and control equipment were used to automatically control mass flow and flow rate of the inlet gases. After being mixed in the mixing chamber, gases entered the reactor were located in the tubular furnace (Atbin, Model ATU 150-15) and temperature was controlled by a digital programmable controller (DPC). The Fischer-Tropsch reaction was carried out in the standard reaction condition of T = 350 and 250 °C, P = 2 bar, H_2/CO = 1/1 and GHSV = 4500 h^{-1}. Product analysis was performed by an on-line gas chromatography using a VARIAN 1400 chromatograph with a thermal conductivity (TCD).

Characterization Techniques

X-ray diffraction. XRD patterns are the techniques to identify crystalline phases by lattice structural parameters, and estimate particle size. Powder diffraction patterns were measured on a Philips PW 1800 diffractometer with operational conditions. Scans were taken with a 2θ step size of 0.02° and a counting time of 1.0 s using a CuKα radiation source generated at 40 KV and 30 mA. XRD samples were prepared by grinding sample in a ring mill until the mean particle size is less than approximately 10 μm. Typical specimens were step integrated at the rate of 4 to 70° per step.

Scanning electron microscopy. A scanning electron microscope is a type of electron microscope that produces images of a sample by scanning it with a focused beam of electrons. The electrons interact with atoms in the sample and produce various signals that can be detected, and that contain information about the sample's surface topography and composition. In this work, SEM was performed with a Mira Tescan instrument to observe the size and particle

morphology while operating at 45 Kv, and samples were gold-coated for producing SEM images.

Nitrogen adsorption (BET method). The values of the surface area and average pore sizes and pore volumes of the catalysts are fundamental properties, which may affect the activity and selectivity of the catalytic reactions. However, surface area is probably the most widely used characterization technique in catalyst synthesis. The surface area of the catalyst precursor, calcined samples (before and after the test), and SiO_2 supports were obtained by the N_2 physisorption using a Quantachrome Nova 2000 automated system. Each catalyst sample was degassed under nitrogen atmosphere at 300 °C for 3 h. The textural characteristics of the analyzed samples were investigated by isothermal gas adsorption/desorption of N_2 at -196 °C for 66 min.

Experimental Results

As mentioned, in this study the silica supported Fe-Co-Ce catalysts were prepared using a wet impregnation procedure. Activity of catalyst was definite as the ability of catalyst to convert input feed to products. It is generally expressed by percentage of carbon monoxide (CO) conversion using Eq. (3):

$$CO\ conversion(\%) = \frac{CO_{in} - CO_{out}}{CO_{in}} \times 100 \qquad (3)$$

where CO_{in} and CO_{out} are the values of input and output of CO to the reactor, respectively. Furthermore, catalyst ability for an arbitrary amount of the desired product was known as the product selectivity calculated by:

$$Selectivity(\%) = \frac{C_p}{CO_{in} - CO_{out}} \times 100 \qquad (4)$$

where C_p is the concentration of the desired product.

RESULTS AND DISCUSSION

Effect of Operational Conditions

The effect of temperature on catalytic performance of experiments were carried out with mixtures of H_2 and CO at a low (250 °C) and high (350 °C) temperatures under the same reaction conditions; H_2/CO feed ratio of 1/1, a

Table 3. Catalytic Performance for FTS in 350 °C Operational Condition of Reaction Temperature
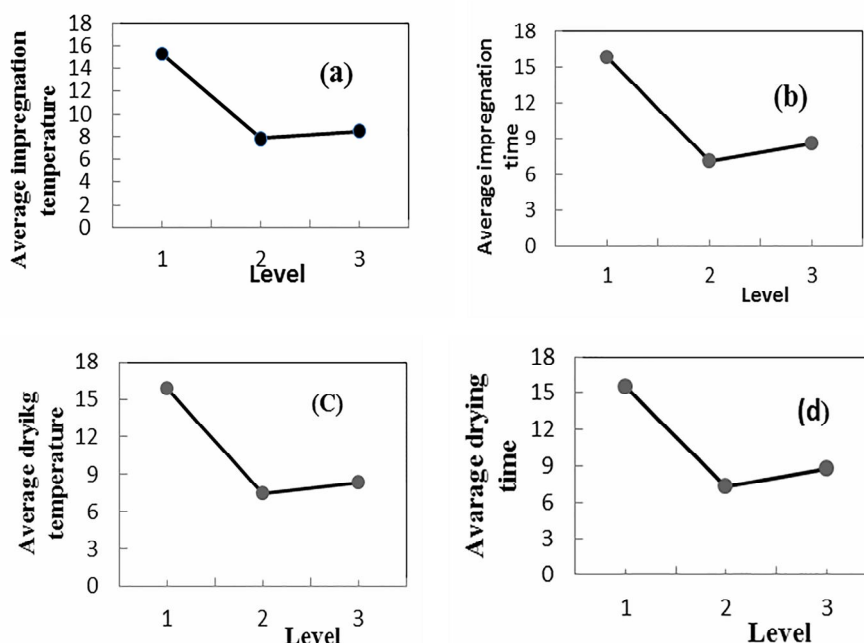
Catalyst number	CO Conversion (%)	Selectivity (%)					
		CH_4	CO_2	C_2H_4	C_2H_6	C_3H_6	C_3H_8
1	30.82	0.13	0.14	0.12	0.61	0	0
2	3.82	0.13	0.14	0.12	0.61	0	0
3	11.01	0.07	0.09	0.01	0.15	0.26	0.01
4	8.85	0.08	0.09	0.02	0.06	0.31	0.01
5	6.91	0.11	0.13	0.22	0	0.17	0.02
6	8.36	0.068	0.06	0.04	0.25	0.25	0.01
7	8.81	0.09	0.11	0.02	0.01	0.34	0.02
8	9.42	0.05	0.06	0.01	0.13	0.25	0.01
9	9.04	0.06	0.06	0	0	0.25	0

Table 4. Catalytic Performance for FTS in 250 °C Operational Condition of Reaction Temperature

Catalyst number	CO Conversion (%)	Selectivity (%)					
		CH_4	CO_2	C_2H_4	C_2H_6	C_3H_6	C_3H_8
1	30.82	0.08	0.51	0.48	0	0	0
2	7.47	0.05	0.03	0	0	0.51	0
3	7.73	0.04	0.03	0	0	0.41	0
4	7.73	0.04	0.03	0	0	0.32	0
5	7.33	0.04	0.02	0	0	0.17	0
6	7.69	0.06	0.02	0	0	0.49	0
7	7.95	0.04	0.02	0	0	0.30	0
8	8.01	0.04	0.02	0	0	0.26	0
9	7.79	0.04	0.02	0	0	0.30	0

Table 5. Average Value as the Optimal Point

Parameter	Level 1	Level 2	Level 3
Impregnation temperature	15.28	7.81	8.5
Impregnation time	15.83	7.16	8.6
Drying temperature	15.85	7.45	8.29
Drying time	15.45	7.35	8.79

Fig. 3. The average value in *versus* levels.

pressure of 2 bar, and the space velocity of 4500 h^{-1}. Results are shown in Tables 3 and Table 4. Under the same operating conditions, the selectivity of light olefin (C$_2$-C$_4$) at 350 °C was higher than the reaction temperature of 250 °C. Because the Fischer-Tropsch polymerization reaction is exothermic, an increase in the reaction temperature always shifts the product towards a lower carbon number. In general, an increase in the reaction temperature leads to an increase in the catalytic performance. Hence, optimum operating temperature for production of light olefins was 350 °C.

Determination of Optimal Level

The data of nine runs at 350 °C were introduced to Minitab software for analysis. The average responses of the factors at different levels are illustrated in Table 5 and used in Fig. 3 (the numbers in the horizontal axis refer to the parameter levels). The aim was to gain the highest carbon monoxide (CO) conversion. As shown in Fig. 3, impregnation temperature of 60 °C (Fig. 3a), impregnation time of 4 h (Fig. 3b), drying temperature of 90 °C (Fig. 3c) and drying time of 6 h (Fig. 3d) were the best conditions to
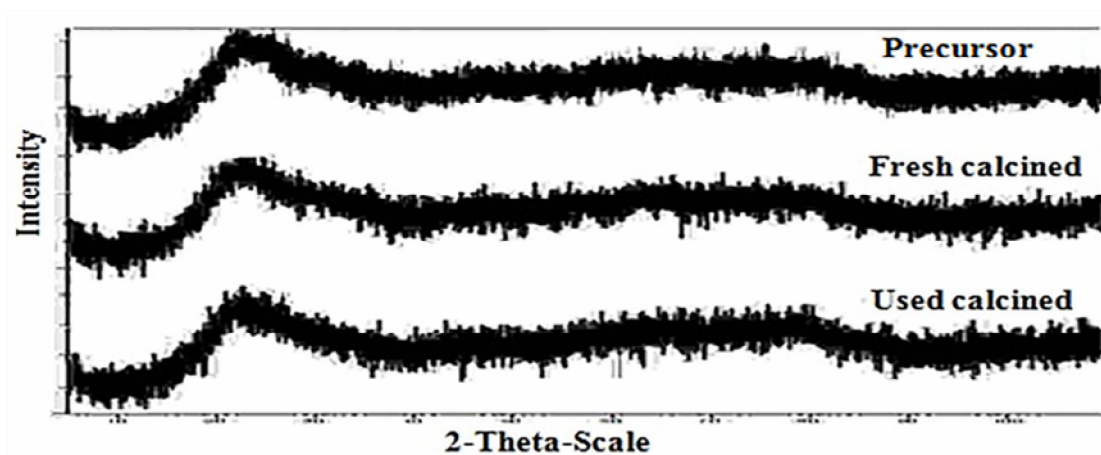
Fig. 4. XRD patterns of precursor and calcined catalysts (before and after the test) containing (33.33%Co/33.33%Fe / 33.33%Ce/ 70wt% SiO$_2$).

Table 6. BET Results of the Precursor and Calcined Catalysts (before and after the Test) Containing (33.33%Co/ 33.33%Fe/33.33%Ce/70wt% SiO$_2$) Prepared with Wet Impregnation Procedure

Specific surface area (m^2 g^{-1})		
Precursor	Fresh calcined	Used calcined
120.42	110.31	322.54

manufacture the catalyst with higher carbon monoxide conversion.

Indeed, performing the impregnation operation in the mild conditions (optimum levels) may lead to better dispersion of metal phase (active sites) on the porous support and increasing the CO conversion. By augmentation of impregnation time, support pores may fill with metal nitrate. Therefore, active site and CO conversion decreased.

Structural Properties of the Catalysts

The XRD technique was carried out to identify the actual phases of optimal catalyst (33.33%Co/33.33%Fe/33.33%Ce/70wt% SiO$_2$) in different states of precursor, fresh calcined (before the test) and used calcined (after the test) catalysts. The XRD patterns of these samples are shown in Fig. 4. In the XRD patterns, a high background in the low-angle region revealed the presence of an amorphous phase in different patterns due to indiscriminate scattering of X-rays. Consequently, other phases may be poorly crystalline or have small crystallite size, and hence have broader peaks in the XRD patterns.

In order to investigate the texture of optimum catalyst, SEM measurement was used. The SEM observations have shown differences in morphology of precursor and desirable calcined catalysts (before and after the reaction). The electron micrograph obtained from catalyst precursor indicates (Fig. 5a) that this material has a less dense and
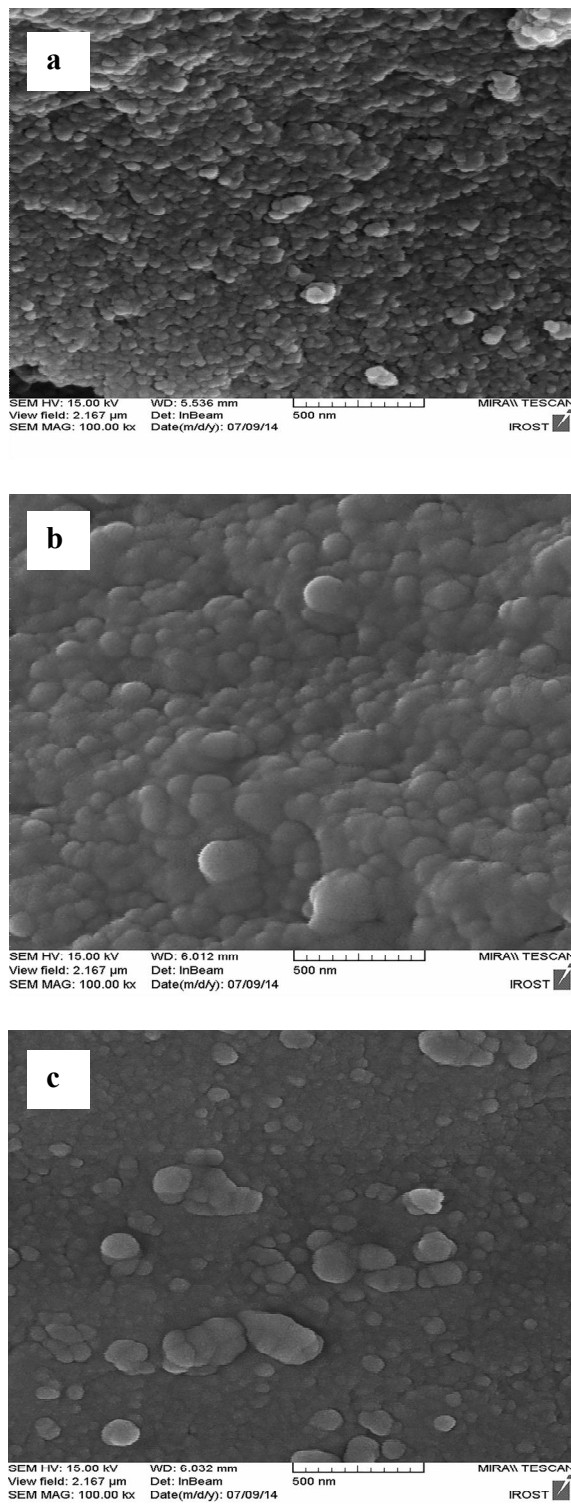
Fig. 5. The SEM observations of precursor and optimal calcined catalyst containing (33.33%Co/ 33.33%Fe/ 33.33%Ce/ 70wt% SiO_2).

homogeneous morphology than the calcined catalyst before the test (Fig. 5b). This difference can be due to the presence of water of crystallization in the structure of the catalyst precursor. Moreover, a comparison between the catalyst after and before the test (Fig. 5c) shows significant differences in the structure and texture and particle size in these two catalysts. Due to sintering and the formation of carbide and metallic phases, particle size is bigger in the tested catalyst (350 °C).

The specific surface area of catalysts (BET) is presented in Table 6. The calcined catalyst after the test has a higher specific surface area (322.54 m^2 g^{-1}) than catalyst precursor (120.41 m^2 g^{-1}) and also the calcined catalyst before the test (110.31 m^2 g^{-1}). According to Table 6, the agglomerate size of calcined catalyst after the test was less compared with its precursor and calcined catalyst before the test; therefore, it led to an increase in the specific surface area of the calcined catalyst after the test. High specific surface area of calcined catalyst after the test allows a high degree of metal dispersion because there are carbide phases.

CONCLUSIONS

In this work, nine catalyst (33.33%Co/33.33%Fe/ 33.33%Ce/70wt% SiO_2) was prepared according to the L_9 orthogonal array. The activity and selectivity of catalysts were evaluated through a fixed-bed micro-reactor, and the effect of operating conditions at 350 °C and 250 °C at the same conditions on the light olefin selectivity was discussed: (feed ratio of H_2/CO = 1/1, a pressure of 2 bar , and the space velocity (GHSV) of 4500 h^{-1}). Optimized conditions were determined by Taguchi method as: 4 h impregnation time, 60 °C impregnation temperature, 6 h drying time, 90 °C drying temperature.

ACKNOWLEDGEMENTS

REFERENCES

[1]   Abdollahi, M.; Atashi, H.; Farshchi Tabrizi , F.; Mansouri, M., Fischer-Tropsch study over impregnated silica-supported cobalt–iron nanocatalyst. *J. Iran. Chem. Soc.,* **2017**, *14*, 245-256, DOI: 10.1007/s13738-016-0975-y.

[2]   Deutschmann, O.; Knözinger, H.; Kochloefl, K.; Turek, T., Heterogeneous catalysis and solid catalysts. Ullmann's Encyclopedia of Industrial Chemistry. 2009, 38-39.

[3]   Mondloch, J. E.; Bayram, E.; Finke, R. G., A review of the kinetics and mechanisms of formation of supported-nanoparticle heterogeneous catalysts. *J. Mol. Catal. A: Chem.* **2012**, *355*, 1-38, DOI: 10.1016/j.molcata.2011.11.011.

[4]   Zohdi-Fasaei, H.; Atashi, H.; Farshchi Tabrizi, F.; Mirzaei, A. A., Exploiting the effects of catalyst geometric properties to boost the formation of light olefins in Fischer-Tropsch synthesis: Statistical approach for simultaneous optimization. *J. Nat. Gas Sci. Eng.* **2016**, *35*, 1025-1031, DOI: 10.1016/ j.jngse.2016.09.040.

[5]   Ryu, J. -H.; Kang, S. -H.; Kim, J. -H.; Lee, Y. -J.; Jun, K. -W., Fischer-Tropsch synthesis on Co-Al_2O_3-(promoter)/ZSM5 hybrid catalysts for the production of gasoline range hydrocarbons. *Korean J. Chem. Eng.* **2015**, *32*, 1993-1998, DOI: 10.1007/ s11814-015-0046-6.

[6]   Mirzaei, A. A.; Shirzadi, B.; Atashi, H.; Mansouri, M., Modeling and operating conditions optimization of Fischer-Tropsch synthesis in a fixed-bed reactor. *J. Ind. Eng. Chem.* **2012**, *18*, 1515-1521, DOI: 10.1016/j.jiec.2012.02.013.

[7]   Fazlollahi, F.; Sarkari, M.; Gharebaghi, H.; Atashi, H.; Zarei, M.; Mirzaei, A. A.; Hecker, W., Preparation of Fe-Mn/K/Al_2O_3 Fischer-Tropsch catalyst and its catalytic kinetics for the hydrogenation of carbon monoxide. *Chin. J. Chem. Eng.* **2013**, *21*, 507-519, DOI: 10.1016/S1004-9541(13)60503-0.

[8]   Arsalanfar, M.; Mirzaei, A. A.; Atashi, H.; Bozorgzadeh, H,; Vahid, S.; Zare, A., An investigation of the kinetics and mechanism of Fischer–Tropsch synthesis on Fe-Co-Mn supported catalyst. *Fuel Process. Technol.* **2012**, *96*, 150-159, DOI: 10.1016/j.fuproc.2011.12.018.

[9]   Zohdi-Fasaei, H.; Atashi, H.; Farshchi Tabrizi, F.; Mirzaei, A. A., Effects of mass transfer on Fischer-Tropsch kinetics over mesoporous silica-supported Co-Mn-Ce nano catalysts in a fixed-bed reactor. *J. Nat. Gas Sci. Eng.* **2016**, *32*, 262-272, DOI: 10.1016/j.jngse.2016.03.090.

[10]   Li, J.; Jacobs, G.; Zhang, Y.; Das, T.; Davis, B. H., Fischer-Tropsch synthesis: effect of small amounts of boron, ruthenium and rhenium on Co/TiO_2 catalysts. *Appl. Catal., A.* **2002**, *223*, 195-203, DOI: 10.1016/S0926-860X(01)00752-9.

[11]   Schulz, H.; Spatial constraints and frustrated reactions in Fischer-Tropsch synthesis. *Catal. Today,* **2003**, *84*, 67-70, DOI: 10.1016/S0920-5861(03)00302-X.

[12]   Luo, M.; Davis, B. H., Fischer-Tropsch synthesis: Group II alkali-earth metal promoted catalysts. *Appl. Catal., A,* **2003**, *246*, 171-181, DOI: 10.1016/S0926-860X(03)00024-3.

[13]   Van Der Laan, G. P.; Beenackers, A. A. C. M., Kinetics and selectivity of the Fischer–Tropsch synthesis: a literature review. *Catal. Rev.* **1999**, *41*, 255-318.

[14]   Riedel, T.; Claeys, M.; Schulz, H.; Schaub, G.; Nam, S. -S.; Jun, K. -W.; Choi, M. -J.; Kishan, G.; Lee, K. -W., Comparative study of Fischer-Tropsch synthesis with H_2/CO and H_2/CO_2 syngas using Fe- and Co-based catalysts. *Appl. Catal., A,* **1999**, *186*, 201-213.

[15]   Zohdi-Fasaei, H.; Atashi, H.; Farshchi Tabrizi, F.; Mirzaei, A. A., Modeling and optimization of Fischer-Tropsch synthesis over $Co-Mn-Ce/SiO_2$ catalyst using hybrid RSM/LHHW approaches. *Energy.* **2017**, *128*, 496-508, DOI: 10.1016/j.energy.2017.03.122.

[16]   Tsakoumis, N. E.; Rønning, M.; Borg, Ø.; Rytter, E.; Holmen, A., Deactivation of cobalt based Fischer-Tropsch catalysts: a review. *Catal. Today,* **2010**, *154*, 162-182, DOI: 10.1016/j.cattod.2010.02.077.

[17]   Van de Loosdrecht, J.; Balzhinimaev, B.; Dalmon, J. -A.; Niemantsverdriet, J.; Tsybulya, S.; Saib, A.; Van Berge, P.; Visagie, J., Cobalt Fischer-Tropsch synthesis: deactivation by oxidation? *Catal. Today,* **2007**, *123*, 293-302, 10.1016/j.cattod.2007.02.032.

[18]   Smitha, S.; Shajesh, P.; Mukundan, P.; Nair, T. D. R.; Warrier, K. G. K., Synthesis of biocompatible hydrophobic silica-gelatin nano-hybrid by sol-gel process. Colloids Surf., B, 2007, 55, 38-43, DOI: 10.1016/j.colsurfb.2006.11.008.

[19]   Adesina, A. A., Hydrocarbon synthesis *via* Fischer-Tropsch reaction: travails and triumphs. *Appl. Catal., A,* **1996**, *138*, 345-367, DOI: 10.1016/0926-860X(95)00307-X.

[20]   Atashi, H.; Zohdi-Fasaei, H.; Farshchi Tabrizi, F.; Mirzaei, A. A., Two-level full factorial design for selectivity modeling and studying simultaneous effects of temperature and ethanol concentration in methanol dehydration reaction, *Phys. Chem. Res.,* **2017**, *5*, 41-56, DOI: 10.22036/pcr.2017.33491.

[21]   Asghari, I.; Esmaeilzadeh, F.; Formation of ultrafine deferasirox particles *via* rapid expansion of supercritical solution (RESS process) using Taguchi approach. *Int. J. Pharm.* **2012**, *433*, 149-156, DOI: 10.1016/j.ijpharm.2012.05.005.

[22]   Milić, J. K.; Petrinić, I.; Goršek, A.; Simonič, M., Ultrafiltration of oil-in-water emulsion by using ceramic membrane: Taguchi experimental design approach. *Cent. Eur. J. Chem.* **2014**, *12*, 242-249, DOI: 10.2478/s11532-013-0373-6.

[23]   Daryapurkar, A.; Kolte, J.; Apte, P.; Gopalan, P., Structural and electrical properties of sodium bismuth titanate ($Na0.5$ $Bi0.5$ TiO_3) thin films optimized using the Taguchi approach. *Ceram. Int.* **2014**, *40*, 2441-2450, DOI: 10.1016/j.ceramint.2013.08.019.

[24]   Karakurt, I., Specific energy optimization in sawing of rocks using Taguchi approach. *J. Central South University.* **2014**, *21*, 365-372, DOI: 10.1007/s11771-014-1949-9.

[25]   Biria, D.; Balouchi, A., Investigation of the role of chemotaxis in bacterial transport through saturated porous media using Taguchi approach. Colloids and Surfaces A: *Physicochem. Engin. Aspects,* **2013**, *436*, 542-548, DOI: 10.1016/j.colsurfa.2013.07.033.

[26]   Ui, S. -W.; Choi, I. -S.; Choi, S. -C., Synthesis of high surface area mesoporous silica powder using anionic surfactant. *ISRN Mater. Sci.,* **2014**, *6*, 2014, DOI: 10.1155/2014/834629.